ALS driven by mutant NEK1 aggregation is accelerated by *Pml* loss, but clinically reversed through pharmacologic induction of *Pml*-mediated degradation

Panagiota Georgiadou [1,2], Bahriye Erkaya [1], Michiko Kawakita [3,4], Egemen Sahin [1], Harun Öztürk [1], Fatmanur Tiryaki [7], Kutay Yildiz [1], Idil Özgenç [1], Emre Pekbilir [1], Sukru Anil Dogan [1], Valérie Lallemand-Breitenbach [3,4], Stephanie Vargas [3,5], Alain Prochiantz [3,5], Elif Nur Firat-Karalar [7], Hugues de Thé [3,4,6]*, Umut Sahin [1,2]*#

[1] Department of Molecular Biology and Genetics, Bogazici University, Istanbul, Turkey

[2] Faculty of Engineering and Natural Sciences, Sabanci University, Istanbul, Turkey

[3] Center for Interdisciplinary Research in Biology (CIRB), Collège de France, CNRS, INSERM, Université PSL, Paris, France

[4] University Paris Cité, INSERM UMR944, CNRS UMR 7212, Institut de Recherche St. Louis, Paris, France

[5] BRAINEVER SAS, 74 rue du Faubourg Saint-Antoine, 75012 Paris, France

[6] Hematology Laboratory, AP/HP, St. Louis Hospital, Paris, France

[7] Koç University, School of Medicine and Department of Molecular Biology and Genetics, Istanbul, Turkey

* Co-senior authors

Corresponding author: umut.sahin@sabanciuniv.edu

H.Ö.'s present address is Northwestern University, Feinberg School of Medicine, Chicago, IL, 60611, USA; F.T.'s and E.P.'s present address is Institute for Molecular

Biology, Mainz, Germany, S.A.D.'s present address is BILSAB, Bezmialem Vakif University

ABSTRACT

Germinal mono-allelic loss-of-function mutations of *NEK1* drive Amyotrophic Lateral Sclerosis (ALS) at variable penetrance, potentially through haploinsufficiency. Modeling the ALS-associated Arg812Ter mutation in mice revealed that the resulting truncated NEK1 ($NEK1^t$) is aggregation-prone, notably in alpha-motoneurons (αMNs), and drives multiple ALS-like symptoms when bi-allelically expressed. Promyelocytic leukemia (*Pml*) is a key genetic interactor, since its loss allows for ALS symptoms to occur even in $Nek1^{wt/t}$ animals, mimicking the human situation. *Pml* precludes disease onset by promoting SUMO-facilitated degradation of $NEK1^t$ proteins. *Pml* upregulation by interferon alpha or poly(I:C) eliminates $NEK1^t$ aggregates in αMNs of $Nek1^{t/t}$ animals, dramatically improving ALS-associated symptoms and extending survival by 6 months. Our study highlights the role of NEK1 aggregates in ALS pathogenesis and identifies interferon or poly(I:C) as a promising candidate therapy acting through *Pml*-triggered degradation of toxic misfolded proteins.

INTRODUCTION

Amyotrophic Lateral Sclerosis (ALS) is a neuromuscular pathology, usually fatal 3-4 years after symptoms onset due to brainstem and spinal alpha-motoneuron (αMN) retrograde degeneration [1]. It is the third most common neurodegenerative disorder in humans, following Alzheimer's and Parkinson's diseases. Early symptoms of ALS include muscle weakness, twitches and cramps. By end stage, patients lose their ability to control voluntary muscles. Death eventually occurs usually because of respiratory failure [2]. Presently, treatment options for ALS are exceedingly limited and lack effectiveness.

Familial ALS forms are caused by mutations in over 30 genes including *SOD1*, *C9orf72*, *FUS* and *TDP43BP* [3]. Understanding the cellular and molecular mechanisms driving disease pathogenesis has been challenging due to the diverse functional and structural nature of the proteins encoded by these genes. *NEK1* is a major ALS-associated gene, with mono-allelic loss-of-function variants in 2-5% of all forms [3-7]. Several ALS-associated *NEK1* mutations introduce premature stop codons, such as Arg812Ter, potentially generating truncated dysfunctional NEK1 variants ($NEK1^t$) (Fig.1A) [4,8]. Recent studies highlighted the importance of defective NEK1 activity in ALS development [9]. As in other neurodegenerative diseases, protein aggregation is a common phenomenon in ALS [10]. Yet, whether misfolding-induced aggregation is implicated in mutant *NEK1*-driven ALS is unclear [3-6,8].

In this study, we simulated the *NEK1* Arg812Ter mutation discovered in ALS patients in mice, revealing a truncated NEK1 protein (truncated NEK1 or $NEK1^t$) highly prone to aggregation, particularly in αMNs. Through this model, we identified the promyelocytic leukemia (*Pml*) gene as a key genetic interactor, protecting mice against disease onset by clearing truncated NEK1 within PML nuclear bodies (NBs). Pharmacological intervention aimed at augmenting *Pml* expression, achieved through interferon alpha (IFN) or poly(I:C) treatment, effectively eliminates $NEK1^t$ and its aggregates from αMNs *in vivo*. This intervention dramatically improves ALS-associated symptoms and survival, in a *Pml*-dependent manner. These findings not only demonstrate the key role of *Pml* to reverse ALS disease progression through degradation of a misfolded protein, but identify interferon or poly(I:C) as a promising therapy for these ALS cases.

RESULTS AND DISCUSSION

Modeling the ALS-linked Arg812Ter mutation in mice reveals a truncated NEK1 ($NEK1^t$) protein

To explore NEK1^{t}-associated ALS, we introduced a point mutation into mouse *Nek1* gene, resulting in a premature stop codon mimicking the human Arg812Ter mutation (Fig.1B) [4]. *Nek1^{t}* heterozygous mice (*Nek1$^{wt/t}$*) showed no significant phenotype (Figs.1C, 1D, 1E, 1F and Supplementary Figs.S1A, S1B), in line with the incomplete ALS penetrance of *NEK1*-mutant human subjects [4,6]. We explored NEK1^{t} expression in mouse tissues, using RT-PCR, Western blot and immunofluorescence (Figs.1G, 1H, 2D and Supplementary Figs.S1C, S1D, S2C). Importantly, *Nek1^{t}* transcripts evade nonsense-mediated decay, leading to truncated protein expression including in αMNs.

ALS-linked NEK1^{t} is largely insoluble and highly prone to aggregation

To clarify the molecular and cellular underpinnings of NEK1^{t}-induced ALS, we expressed the GST- or GFP-tagged human mutant protein in HEK293 or Neuro2A cells. While wild-type NEK1 protein (wtNEK1) exhibits a diffuse cytoplasmic expression pattern (Supplementary Fig.S1E) [11,12], NEK1^{t} is confined to the nucleus, reflecting the loss of two nuclear export sequences (Fig.1A and Supplementary Fig.S1E) [4]. Within nuclei, NEK1^{t} forms aggregate-like structures reminiscent of phase-separated Tau, α-synuclein, or TDP-43 aggregates (Supplementary Fig.S1E) [13,14]. Nearly 80% of NEK1^{t}-expressing cells present nuclear aggregates in both cell types, while none are observed in wtNEK1-expressing cells (Supplementary Fig.S1E). Real-time video-microscopy revealed that GFP-NEK1^{t} rapidly forms nuclear aggregates (Supplementary Fig.S1F). Fluorescence recovery after photobleaching (FRAP) analyses of GFP-NEK1^{t} aggregates showed poor fluorescence recovery (Supplementary Fig.S1G), indicating a non-dynamic gel-like state, consistent with other phase-separated protein aggregates [13,14]. Accordingly, a sequential protein fractionation assay demonstrated predominantly insoluble NEK1^{t}, contrary to soluble wtNEK1 (Fig.1I).

***Pml* mitigates ALS emergence through PML nuclear body-mediated, SUMO-facilitated degradation of NEK1^t**

Investigating potential genetic interactors of *Nek1^t*, we focused on *Pml*, as PML organizes nuclear bodies (NBs) that regulate the stability of client proteins through SUMOylation and ubiquitylation [15-17]. *Pml$^{-/-}$* mice exhibit no notable physiological symptoms, presenting a normal lifespan [18,19]. Yet, PML may facilitate proteolysis of misfolded DRIPs or mutant proteins [17,20]. Strikingly, *Nek1$^{wt/t}$* animals in a *Pml* knockout background (*Nek1$^{wt/t}$ Pml$^{-/-}$*) now showed an ALS-like phenotype, characterized by severe muscle weakness, impaired coordination and motor function, starting 31.5 weeks post-birth or later, as measured by grip strength and hanging wire analyses (Figs.1E, 1F and Supplementary Fig.S1B). They also showed weight loss (Fig.1D) and a markedly shortened lifespan (Fig.1C) though this phenotype was not fully penetrant. Thus, *Pml* absence *in vivo* reveals ALS-like pathogenesis fueled by heterozygous NEK1^t expression.

Interferons enhance PML NB biogenesis, driving the recruitment of client proteins into these structures, subsequently promoting client *in situ* SUMOylation, as well as their STUbL-mediated ubiquitylation and proteasomal degradation [17]. Remarkably, a fraction of NEK1^t co-localized with PML in NBs in the basal state (Figs.1J, 1K and Supplementary Fig.S1H). Interferon alpha (IFNα)-mediated recruitment of NEK1^t into NBs was accompanied by its conjugation by SUMO1 and SUMO2/3 (Figs.1K, 2A and Supplementary Fig.S1H), precipitating NEK1^t's proteasome- and PML-dependent degradation (Figs.2B, 2C and Supplementary Fig.S2A), ultimately clearing NEK1^t aggregates in transfected cells (Supplementary Fig.S2B). PML thus degrades this mutant protein, likely explaining the emergence of ALS symptoms in *Pml* null *Nek1$^{wt/t}$* mice. Accordingly, IFNα therapy may benefit NEK1^t-driven ALS.

We then explored *Nek1*^{t} homozygous mice (*Nek1*$^{t/t}$) where increased NEK1^{t} abundance and/or some defects in NEK1 functions allowed for rapid development of ALS-like phenotypes even in *Pml* proficient mice, causing death (median survival 35 weeks) (Figs.1C, 1D, 1E, 1F and Supplementary Figs.S1A, S1B). Beyond ALS-like phenotypes, *Nek1*$^{t/t}$ displayed other symptoms, including dwarfism, polycystic kidneys, and male sterility (Supplementary Fig.S1A, data not shown), reflecting ciliopathy likely linked to loss of NEK1 functions [11,21-24]. Moreover, *Nek1*$^{t/t}$ mice present large numbers of NEK1^{t} aggregates within spinal cord αMNs, something never observed in wild-type or *Pml* proficient *Nek1*$^{wt/t}$ animals (Figs.1G, 1H and Supplementary Figs.S1C, S1D). To explore any accelerating role of *Pml* loss, we generated *Nek1*$^{t/t}$ animals in a *Pml*$^{-/-}$ background. These mice displayed exacerbated muscle weakness and accelerated weight loss, succumbing to disease a week earlier than *Pml* proficient *Nek1*$^{t/t}$ mice (Figs.1C, 1D, 1E, 1F and Supplementary Fig.S1B). We also observed a slightly increased number of NEK1^{t} aggregates in their αMNs (Supplementary Fig.S1I). Overall, these findings demonstrate that NEK1^{t} drives an ALS-like phenotype, a process normally prevented by PML, most likely through basal SUMOylation-induced NEK1^{t} degradation.

Pml targeting _in vivo_ clears NEK1^{t} aggregates from alpha-motoneurons, alleviates disease symptoms and improves survival

We then assessed any potential therapeutic benefit of *Pml* gene induction by IFNα on NEK1^{t}-driven ALS-like phenotype *in vivo*. Following IFNα or poly(I:C) therapy of pre-symptomatic animals initiated 5 weeks post-birth, treated *Nek1*$^{t/t}$ mice exhibited elimination of the NEK1^{t} proteins from multiple tissues, including spinal cord, with the expected reduction of NEK1^{t} aggregates in αMNs (Figs.2D, 2E and Supplementary Fig.S2C). In contrast, wtNEK1 was unaffected by IFNα or poly(I:C) therapy (Supplementary Fig.S2D). Strikingly, IFNα- or poly(I:C)-treated *Nek1*$^{t/t}$ mice

exhibited mild or no symptoms for several months and succumbed to ALS much later (median survival 58 weeks, compared to 35 weeks in untreated *Nek1*$^{t/t}$ mice) (Figs.2F, 2G and Supplementary Fig.S2E). Critically, the same IFNα or poly(I:C) regimen failed to mitigate ALS-like symptoms or extend survival in *Nek1*$^{t/t}$ *Pml*$^{-/-}$ animals (Figs.2F, 2G and Supplementary Fig.S2E) or to clear NEK1^{t} from tissues (Fig.2D and Supplementary Fig.S2C). Overall, IFNα or poly(I:C) therapy extended survival by 6 months, alleviating ALS-like symptoms throughout treatment, a process requiring *Pml* and associated to *Pml*-driven clearance of the mutant protein in spinal cord αMNs.

NEK1 mutations represent ALS-risk variants for 2-5% of sporadic and familial forms [3-6,8]. While the role of nuclear NEK1^{t} aggregation in ALS remains uncertain, evidence presented here identifies a tight correlation between the expression of the truncated protein, the occurrence of aggregates in αMNs, ALS-like symptoms and disease progression. Conversely, eliminating NEK1^{t} from αMNs through IFNα- or poly(I:C)-induced *Pml*, yields disappearance of ALS-like symptoms, resulting in sharp survival benefits, despite expected defects in NEK1 function. To our knowledge, this is the most dramatic benefit ever reported in treatment trials initiated pre-symptomatically in ALS mouse models. Thus, *Pml* induction drives clearance of a misfolded protein in a neurodegenerative disease *in vivo* with a striking clinical benefit, while *Pml* absence allows emergence of the disease in *Nek1*$^{wt/t}$ mice. These studies highlight the contribution of toxic aggregates to ALS, in addition NEK1 dysfunction(s). *NEK1* alterations are often found together with other susceptibility genes (i.e. *C9orf72, TARDBP*) that yield toxic protein aggregates, which could reflect a mutual facilitation of phase separation [5,6,25-27]. *Pml*-induced clearance of misfolded proteins upon IFNα or poly(I:C) therapy could be effective for other mutant proteins associated to ALS or other neuro-degenerative diseases eligible for *Pml* interaction. In that respect, PML was proposed to facilitate

degradation of mutated ataxin-1, Huntingtin and TDP-43 proteins *in vitro* [20]. In SCA1 mice, *Pml* absence enhances pathological brain lesions, but not clinical phenotype [20]. Thus, the results reported here may have broader implications than ALS associated with this specific NEK1 mutation. Our study is the first to show, *in vivo*, a dramatic Pml-dependency of mutant protein stability and aggregation, disease incidence, as well as a provocative Pml-dependent clinical response to interferon. Our findings also provide a novel conceptual understanding of ALS pathogenesis, as well as some support to the "hygiene hypothesis," explaining the rising incidence of neurodegenerative disorders in societies with high hygiene standards. Indeed, infections may exert protective effects through repeated activation of interferon signaling, clearing toxic protein aggregates in the central nervous system.

MATERIALS AND METHODS

Creation of a *Nek1^t* ALS mouse model, genotyping, RNA and protein analyses

The mouse NEK1-Lys764Ter mutation corresponds to the human NEK1-Lys812Ter mutation found in a subset of ALS patients and results in the expression of the truncated NEK1^t protein. NEK1-Lys764Ter mutant mice and *Pml* deficient (*Pml$^{-/-}$*) mice were created using the i-GONAD method [28]. CRISPR/Cas9 reagents were injected into the oviducts of pregnant FVB/N females, followed by electroporation (NEPA21 Electroporator, Sonidel) of the entire oviduct. crRNA, tracrRNA, ssDNA, and Cas9 nuclease were purchased from IDT (Integrated DNA Technologies). For NEK1-Lys764Ter mutation, the CRISPR target sequence (without PAM) was 5'-AACATACTCATACATACTTT-3'

and the ssODN sequence was 5'-GATGCAGTGACACTGGATACATCCTTCTCTGCAACCGAATGTATGTATGAGTATGTTAATGTCATGGCTTGGTTTATCAC-3'. For *Pml$^{-/-}$* animals, the CRISPR target sequence (without PAM) was 5'- GTGTTGCACATGCGCGCTCC -3'.

Genotyping was performed by PCR and direct DNA sequencing for each animal. Earpieces were obtained from 3-week-old mice, after separation from their mothers. DNA extraction buffer containing proteinase K in a 1:100 ratio (20mg/ml, GoldBio, Cat # P-480-100) was added to each sample and left for overnight incubation in a shaking block (600rpm, at 58°C). The following day the samples were taken and following a series of washes with isopropanol and ethanol, genomic DNA was obtained and used for PCR reactions at the following conditions: Initial denaturation 95°C for 30 sec; [95°C for 30 sec, 60°C for 30 sec, 72°C for 45 sec]X34; final extension 68°C for 5 min. The following PCR primer sets were used:

Nek1-Forward 5'-ATACCCAGGAAGAAGAAATGGAAA-3;

Nek1-Reverse 5'- GCCACTGCAAAGACCAAACTT-3;

Pml-Forward 5'-GGTTGTCAGACTTGGCTGTGA-3;

Pml- Reverse 5'-GCAGCTGGACTTTCTGGTTCT-3'.

PCR with *Nek1*-Forward and *Nek1*-Reverse primers generates a 524bp fragment. The purified PCR product was then sequenced using Nek1-sequencing primer Fwd: 5'- GTGCTATTTCAGTAAGTACAG -3'. PCR with *Pml*-Forward and *Pml*-Reverse primers generates a 671bp fragment in wild-type animals and a 612bp fragment in the knockouts.

The expression of *Nek1* and *Nek1*^{t} transcripts were verified by RT-PCR. RNA was isolated from from various mouse tissues using Direct-Zol RNA Isolation Kit (Zymogen, Cat # R2071). cDNA synthesis was performed using SensiFAST cDNA Synthesis Kit (Bioline, Cat # BIO-65053) according to manufacturer's instructions. PCR was performed using primers specific for *Nek1* and *Gapdh* sequences. A set of primers was used to amplify a 167 bp-long shared region present in both wild-type and *Nek1*^{t} transcripts. The following PCR primers sets were used:

Nek1-Forward 5'- TGGCAAACATGAAGCATCCA -3';

Nek1-Reverse 5'- CACAAACCAGTCCAAAATCTGG -3';

Gapdh-Forward 5'- AAGGGCTCATGACCACAG - 3';

Gapdh-Reverse 5' - CATCACGCCACAGCTTTCC -3'

(*Gapdh* was used as an internal control). The following PCR protocol was employed (initial denaturation 95°C for 30 sec; [95°C for 30 sec, 60°C for 20 sec, 72°C for 15 sec]X34; final extension 68°C for 5 min).

For protein and Western blot analysis, mouse spinal cord and heart tissues were removed and lysed in organic lysis buffer containing 50mM HEPES, 1% Triton X-100, 10mM EDTA, 2% SDS and 50mM NaCl. Protein lysates were mixed with 2X *L*aemmli buffer and boiled for 5 min at 70°C prior to SDS-PAGE. The following antibodies were used for the detection of proteins: human anti-NEK1 (Santa Cruz, Cat # sc-398813**),** human anti-GAPDH (Santa Cruz, Cat # sc-32233).

Motor function tests

Grip strength tests (Ugo Basile, Cat # 47200) measure the maximum force that a mouse can exert on an apparatus, hence measuring muscle strength and overall neuromuscular function, documenting any possible muscle weakness. Each animal was placed on a base plate, being pulled by the tail. Three different measurements (of the force exerted, indicated on y-axes as gram force, gf) were taken for each animal, and the averages were calculated. The weekly scores of each animal were normalized to weight. Animals were subjected to the test starting at week 6 after birth.

For hanging wire tests, animals were allowed to hang on a wire and the time they were active and moving was recorded (indicated on y-axes as motility, units are in seconds, sec), within a timeframe of 4 minutes in total.

The onset of ALS symptoms was evaluated through multiple factors, including decline in muscle strength and overall neuromuscular function (measured by grip strength and hanging wire tests), motor deficits and coordination loss (assessed via rotarod and clasping tests, data not shown), and weight loss. A 20% reduction in muscle strength was considered the onset of symptoms.

In vivo treatments

Mice were injected intraperitoneally with 10000 U of recombinant mouse interferon alpha (IFNα) (Sino Biological, Cat # 50525-M01H) in 100µl of vehicle containing murine serum albumin (MSA, Sigma Aldrich) at 1mg/ml in PBS pH 7.0, three times a week starting at 5 weeks of age. Treatment was continued over the lifespan of animals (or until sacrifice). Similarly, as an alternative, to induce the activation of endogenous interferon signaling *in vivo* [29], the animals received intraperitoneal injections of poly(I:C) (Invivogen, Cat # 31852-29-6) twice a week, beginning at week 5 after birth, at a dosage of 20µg per gram for the duration of their lifetime. We observed that IFNα and poly(I:C) had equivalent *in vivo* effects on survival and therapeutic benefit.

Immunofluorescence on tissues

Animals were sacrificed in a CO_2 chamber and the spinal cords were obtained after dissection, followed by fixation in 4% paraformaldehyde for an hour at 4°C, then overnight incubation in 20% sucrose for better cryoprotection. Tissues were subsequently embedded in molds filled with OCT (embedding matrix, VWR, Cat # 65608-930) and frozen. Tissue sections were obtained in 30µM thickness using Cryostar NX 70 cryostat. Immunofluorescence was performed on tissue sections following cytoplasmic and nuclear permeabilization of this highly myelinated tissue.

For this, after washing away the OCT using PBS, slides were placed in 2% Triton X-100 in PBS for 30 min at room temperature to remove the myelin, followed by the "heat shock demasking" step, performed by incubation in citrate buffer (0.1M citric acid and 0.1M sodium citrate, pH 6.0) for 20 min at 90°C. Following subsequent incubation in PBS containing 3% H_2O_2 and 10% methanol for 15 min at room temperature, the tissues were permeabilized in 0.5% Triton X-100 (1 hr at room temperature). Next, slides were washed in PBS and then incubated in 100mM glycine, washed again in PBS and finally placed in a blocking buffer containing 1% Fetal Bovine Serum (Gibco, Cat # 10270106) and 1% Triton X-100. Primary antibody incubation was performed overnight +4°C.The next day slides were washed three times in PBS containing 0.1% Triton X-100 and incubated with secondary antibodies for 2 hrs at room temperature. After washing three times in PBS, slides were mounted in DAPI (Southern Biotech, Cat # 0100-20**).** The following antibodies were used: human anti-NEK1 antibody (Santa Cruz, Cat # sc-398813) and anti-VAChT (Sigma-Aldrich, Cat # ABN100). Images were obtained using a confocal microscope (Leica TCS SP8, USA) and analyzed using Image J, Fiji and LASX software packages. Alpha-motoneurons were detected based on size and VAChT expression.

Cell culture, constructs, transfections and treatments

HEK293 or Neuro2A cells were maintained in DMEM supplemented with 10% FBS and 1% penicillin/streptomycin. Cells were kept in a humidified incubator that maintained the temperature at 37°C and CO_2 levels at 5%. The expression plasmid for the GST-tagged human NEK1 was purchased from Addgene. In order to generate the NEK1^{t} mutant, which contains a premature stop codon at amino acid position 812, site directed mutagenesis was performed on the abovementioned plasmid using the following primers:

Arg812Ter-Forward: 5'-CTACAACTGAATGACATACAGTG-3';

Arg812Ter-Reverse: 5'-CACTGTATGTCATTCAGTTGTAG-3'

Plasmids encoding SUMO proteins were described previously [17,30]. The day before plasmid DNA transfection, HEK293 cells were seeded as they reach 50-70% confluency at the time of transfection. 500ng or 1µg plasmid DNA were transfected into cells grown in 12- and 6-well plates, respectively. For transfection to 12-well plates, the plasmid DNA was dissolved in water. Then 30.5µl of 2M ice-cold $CaCl_2$ was added to the mixture, followed by dropwise addition of 250µl 2x HBS (Lonza, Cat # CC-5024). After 10 min incubation, transfection mix was gently added to the cells.

siRNA transfections of HEK293 cells were performed using HiPerFect transfection reagent (Qiagen, Cat # 301705), according to manufacturer's instructions. The siRNA sequence used to silence Pml expression was 5'-AAGAGTCGGCCGACTTCTGGT-3'. The control (non-targeting) siRNA sequence used in the same experiment was 5'-UUCUCCGAACGUGUCACGUTT-3'.
Neuro2A cells were transfected using the Metafectene reagent (Biontex, Cat # T020-1.0), according to manufacturer's instructions.

HEK293 cells were treated with recombinant human interferon alpha (PBL Assay Science, Cat # 11100-1) for 24 hours at a concentration of 1000 U/ml. MG132 (Hycultec, Cat # HY-13259) treatment was performed at a final concentration on 1µM. Neuro2A cells were treated with recombinant mouse interferon alpha (Sino Biological, Cat # 50525-M01H) for 24 hours at a concentration of 1000 U/ml.

The following antibodies were used for Western blots in HEK293 or Neuro2A cells:
anti-GST (Cell signaling, Cat # 2624S), human anti-GAPDH (Santa Cruz, Cat # sc-32233;), human anti-actin (BioLegend, Cat # 622102), human anti-YY1 (Santa Cruz, H-10, Cat # sc-7341), human anti-PML (Santa Cruz, H-238, Cat # sc-5621 and Santa

Cruz, E-11, Cat # sc-377390), human anti-SUMO1 (CST, Cat # 4930), human anti-SUMO2/3 (Abcam, Cat # ab3742).

Immuno-precipitations and SUMOylation assays

SUMOylation assays on NEK1 or NEK1^{t} proteins were performed as described previously [17,30,31], following transfection of HEK293 cells with plasmids encoding the GST-tagged versions of these proteins and/or SUMO1 or SUMO2 proteins. Cells were treated with recombinant human interferon alpha (PBL Assay Science, Cat # 11100-1) for 24 hours at a concentration of 1000 IU/ml. An anti-GST antibody (Cell Signaling, Cat # 2624S) was used for immunoprecipitation.

Solubility Assay

In order to assess the solubilities of wild-type and NEK1^{t} proteins, plasmids encoding these proteins were expressed in HEK293 cells. Cells were collected 48 hrs post-transfection and lysed in 150 µl NP40-containing buffer (50mM Tris-HCl pH 8.0, 150mM NaCl, 1% NP40) by incubation for 30 min on ice. Next, the supernatant was collected after centrifuging the samples at 13000 rpm for 20 minutes at 4°C (this is the NP40-soluble fraction) and mixed with 50µl 4x Laemmli buffer and boiled. The remaining pellet was lysed by boiling in 10 µl of 2x Laemmli buffer (this is the SDS-soluble fraction). Samples were subsequently analyzed by Western blotting. YY1 is a nuclear protein (transcription factor) and was used as a positive control to demonstrate that the NP40-based lysis conditions that we used allowed extraction of soluble nuclear proteins.

Immunofluorescence, confocal microscopy, FRAP and live cell imaging

The following antibodies were used for immunofluorescence on HEK293 or Neuro2A cells: human anti-GST (Cell Signaling, Cat # 2624S), human anti-FLAG (Sigma, Cat # F1804). Coverslips were placed in 12-mm culture dishes where HEK293 or

Neuro2A cells were seeded. Cells were fixed in 4% PFA solution (20 min at room temperature). Following 2 rinses in cold PBS, cells were permeabilized in 0.25% Triton X-100 (15 min). They were then washed 3 times with PBS (5 min each) and blocked in 1% BSA (in PBS-Tween) for 1 hr. Primary antibody incubation was performed in blocking solution for 1 hr at room temperature in a humidified chamber, followed by 3 washes in PBS-Tween (5 min each). Secondary antibody incubation was performed in blocking solution for 1 hr at room temperature, this time in dark, followed by 3 washes in PBS-Tween (5 min each). Next, cells were incubated in DAPI (1 µg/ml, Southern Biotech, Cat # 0100-20) for 3 min, which was followed by rinsing in PBS. Coverslips were mounted on slides using the fluoroshield mounting medium. Images were acquired using a confocal microscope (Leica TCS SP8, USA) and analyzed using Image J, Fiji and LASX software packages.

For real-time microscopy analyses, a Leica SP8 confocal microscope with an incubation chamber was used. Unsynchronized cells were analyzed at 37°C in a 5% CO_2 atmosphere at 0.375-second intervals in a 512x512 pixel format using an HC PL APO CS2 40x 1.3 NA objective.

For deconvoluted confocal analysis, high-resolution images were captured using an HC PL APO 100x/1.4 NA CS2 objective and deconvoluted with Huygens software.

For fluorescence recovery after photobleaching (FRAP) analyses, the FRAP module on the Leica SP8 microscope was used. Bleaching (fluorescence signal elimination) was performed with a 488 Argon laser at 100% power capacity. Images were captured using Leica LASX software and analyzed with Image J.

Statistical analyses

For Fig.1C, animals from five different genotypes were monitored for a thorough lifespan comparison. The groups included 12 wild-type, 14 *Nek1*$^{wt/t}$, 22 *Nek1*$^{t/t}$, 18 *Nek1*$^{wt/t}$ *Pml*$^{-/-}$ and 27 *Nek1*$^{t/t}$ *Pml*$^{-/-}$ animals. Statistical analysis was performed using the Log-Rank (Mantel-Cox) and Gehan Generalized Wilcoxon Tests. For Fig.1D, the weights of animals from five different genotypes were monitored up to week 70 after birth (or until their week of death). For each group, ≥7 animals were included in the analysis. Statistical analysis was performed using the Student's t-test (paired). ALS-associated weight loss in *Nek1*$^{t/t}$ mice (16.4%) was accelerated in *Pml* absence (20%), as calculated by animals' weight at week of death (indicated by a cross) versus maximal weight attained (week 25). *Nek1*$^{wt/t}$ *Pml*$^{-/-}$ mice, but not *Nek1*$^{wt/t}$, also exhibit weight loss starting at weeks 60/70. In Figs.1F and 2G, each data point corresponds to the average of measurements from at least five different animals for a given week, with a minimum of three animals used at very late time points as some animals begin to die. In Fig. 2F, animals from two different genotypes that received therapy or not were monitored for survival comparison. The groups included 22 *Nek*$^{t/t}$, 27 *Nek1*$^{t/t}$ *Pml*$^{-/-}$, 11 *Nek*$^{t/t}$ receiving IFN/poly(I:C) and 7 *Nek1*$^{t/t}$ *Pml*$^{-/-}$ receiving IFN/poly(I:C). At the time of submission, one 52-week-old *Nekl1*$^{t/t}$ mouse receiving therapy was still alive and in good condition, and was included in the Kaplan Meier survival probability calculations. Statistical analysis was performed using the Log-Rank (Mantel-Cox) and Gehan Generalized Wilcoxon Tests. For the quantifications of aggregates in motor neurons and transfected cells, as well as of protein abundances in Western blots, statistical analyses were performed using the Student's t-test (unpaired, assuming unequal variances). The asterisks indicate the following p-values: (*) <0.05, (**) <0.01, (***) <0.001, (****) <0.0001.

REFERENCES

1. Mead, R.J., Shan, N., Reiser, H.J., Marshall, F. & Shaw, P.J. Amyotrophic lateral sclerosis: a neurodegenerative disorder poised for successful therapeutic translation. *Nat Rev Drug Discov* **22**, 185-212 (2023).

2. Taylor, J.P., Brown, R.H., Jr. & Cleveland, D.W. Decoding ALS: from genes to mechanism. *Nature* **539**, 197-206 (2016).

3. Nguyen, H.P., Van Broeckhoven, C. & van der Zee, J. ALS Genes in the Genomic Era and their Implications for FTD. *Trends Genet* **34**, 404-423 (2018).

4. Brenner, D.*, et al.* NEK1 mutations in familial amyotrophic lateral sclerosis. *Brain* **139**, e28 (2016).

5. Jiang, Q.*, et al.* Genetic and clinical characteristics of ALS patients with NEK1 gene variants. *Neurobiol Aging* **123**, 191-199 (2023).

6. Kenna, K.P.*, et al.* NEK1 variants confer susceptibility to amyotrophic lateral sclerosis. *Nat Genet* **48**, 1037-1042 (2016).

7. Cirulli, E.T.*, et al.* Exome sequencing in amyotrophic lateral sclerosis identifies risk genes and pathways. *Science* **347**, 1436-1441 (2015).

8. Higelin, J.*, et al.* NEK1 loss-of-function mutation induces DNA damage accumulation in ALS patient-derived motoneurons. *Stem Cell Res* **30**, 150-162 (2018).

9. Mann, J.R.*, et al.* Loss of function of the ALS-associated NEK1 kinase disrupts microtubule homeostasis and nuclear import. *Sci Adv* **9**, eadi5548 (2023).

10. Malik, R. & Wiedau, M. Therapeutic Approaches Targeting Protein Aggregation in Amyotrophic Lateral Sclerosis. *Front Mol Neurosci* **13**, 98 (2020).

11. Chen, Y.*, et al.* Expression of Nek1 during kidney development and cyst formation in multiple nephron segments in the Nek1-deficient kat2J mouse model of polycystic kidney disease. *J Biomed Sci* **21**, 63 (2014).

12. Chen, Y., Chen, C.F., Riley, D.J. & Chen, P.L. Nek1 kinase functions in DNA damage response and checkpoint control through a pathway independent of ATM and ATR. *Cell Cycle* **10**, 655-663 (2011).

13. Elbaum-Garfinkle, S. Matter over mind: Liquid phase separation and neurodegeneration. *J Biol Chem* **294**, 7160-7168 (2019).

14. Zbinden, A., Perez-Berlanga, M., De Rossi, P. & Polymenidou, M. Phase Separation and Neurodegenerative Diseases: A Disturbance in the Force. *Dev Cell* **55**, 45-68 (2020).

15. Lallemand-Breitenbach, V. & de The, H. PML nuclear bodies: from architecture to function. *Curr Opin Cell Biol* **52**, 154-161 (2018).

16. Celen, A.B. & Sahin, U. Sumoylation on its 25th anniversary: mechanisms, pathology, and emerging concepts. *FEBS J* **287**, 3110-3140 (2020).

17. Sahin, U.*, et al.* Oxidative stress-induced assembly of PML nuclear bodies controls sumoylation of partner proteins. *J Cell Biol* **204**, 931-945 (2014).

18. Wang, Z.G.*, et al.* PML is essential for multiple apoptotic pathways. *Nat Genet* **20**, 266-272 (1998).

19. Hsu, K.S. & Kao, H.Y. PML: Regulation and multifaceted function beyond tumor suppression. *Cell Biosci* **8**, 5 (2018).

20. Guo, L.*, et al.* A cellular system that degrades misfolded proteins and protects against neurodegeneration. *Mol Cell* **55**, 15-30 (2014).

21. Upadhya, P., Birkenmeier, E.H., Birkenmeier, C.S. & Barker, J.E. Mutations in a NIMA-related kinase gene, Nek1, cause pleiotropic effects including a progressive polycystic kidney disease in mice. *Proc Natl Acad Sci U S A* **97**, 217-221 (2000).

22. El Hokayem, J.*, et al.* NEK1 and DYNC2H1 are both involved in short rib polydactyly Majewski type but not in Beemer Langer cases. *J Med Genet* **49**, 227-233 (2012).

23. Monroe, G.R.*, et al.* Compound heterozygous NEK1 variants in two siblings with oral-facial-digital syndrome type II (Mohr syndrome). *Eur J Hum Genet* **24**, 1752-1760 (2016).

24. Thiel, C.*, et al.* NEK1 mutations cause short-rib polydactyly syndrome type majewski. *Am J Hum Genet* **88**, 106-114 (2011).

25. Riva, N.*, et al.* NEK1 Variants in a Cohort of Italian Patients With Amyotrophic Lateral Sclerosis. *Front Neurosci* **16**, 833051 (2022).

26. Rifai, O.M.*, et al.* Clinicopathological analysis of NEK1 variants in amyotrophic lateral sclerosis. *Brain Pathol*, e13287 (2024).

27. Guo, Q.*, et al.* In Situ Structure of Neuronal C9orf72 Poly-GA Aggregates Reveals Proteasome Recruitment. *Cell* **172**, 696-705 e612 (2018).

28. Ohtsuka, M. & Sato, M. i-GONAD: A method for generating genome-edited animals without ex vivo handling of embryos. *Dev Growth Differ* **61**, 306-315 (2019).

29. Tessier, S.*, et al.* Exploration of nuclear body-enhanced sumoylation reveals that PML represses 2-cell features of embryonic stem cells. *Nat Commun* **13**, 5726 (2022).

30. Ergunay, T.*, et al.* Sumoylation of Cas9 at lysine 848 regulates protein stability and DNA binding. *Life Sci Alliance* **5**(2022).

31. Auvin, S.*, et al.* A molecule inducing androgen receptor degradation and selectively targeting prostate cancer cells. *Life Sci Alliance* **2**(2019).

ABBREVIATIONS

ALS: amyotrophic lateral sclerosis

DRIPs: defective ribosomal products

GFP: green fluorescent protein

IFNα: interferon alpha

αMN: alpha-motoneuron

NB: nuclear body

PML: promyelocytic leukemia

poly(I:C): polyinosinic:polycytidylic acid

SCA1: spinocerebellar ataxia type 1

SCA7: spinocerebellar ataxia type 7

SUMO: small ubiquitin-like modifier

STUbL: SUMO-targeted ubiquitin ligase

TDP43: TAR DNA-binding protein 43

FIGURE LEGENDS

Figure 1: *Pml* safeguards against development of ALS driven by a truncated NEK1 mutant aggregating in αMNs. **A)** NEK1^t domain structure compared with wild-type NEK1. CC: coiled coil. NES: nuclear export sequence. **B)** Genomic location of the point mutation introduced in the mouse *Nek1* gene, compared to ALS patients. Amino acids in bold. **C)** Survival of *Pml*-proficient or -deficient *Nek1*$^{wt/t}$ or *Nek1*$^{t/t}$ mice. **D)** Evolution of weight in mutant mice. Cross denotes death. **E)** Summary of the ALS-like symptoms. Evaluation of disease onset in (Materials and Methods). **F)** Muscle strength and neuromuscular functions (grip strength and hanging wire). Trendlines are in Supplementary Fig.S1B. **G)** Western blot illustrating NEK1^t protein expression in spinal cords of animals with the indicated genotypes (*) wtNEK1, (**) NEK1^t..**H)** Immunofluorescence showing NEK1 protein in *wild-type* (top), *Nek1*$^{wt/t}$ (middle) or NEK1^t aggregates in *Nek1*$^{t/t}$ (bottom) spinal cord αMNs, identified by VAChT expression. Number of nuclear or cytoplasmic aggregates (30 αMNs from 3 mice). **I)** Assessment of NEK1^t protein solubility, in NP40, then SDS, in transiently transfected HEK293 cells. **J)** Recruitment of transfected GFP-NEK1^t into PML NBs (confocal image with deconvolution). **K)** IFNα enhances NEK1^t co-localization with PML in transfected HEK293 cells (n=3). Representative images in Supplementary Fig.S1H.

Figure 2: Therapeutic benefit of *Pml* induction by IFNα or poly(I:C) through NEK1^t clearance *in vivo*. **A)** NEK1^t modification by SUMO1 and SUMO2/3. HEK293 cells were transfected with the indicated expression vectors and treated or not with IFNα. IP: immuno-precipitation, WCL: whole cell lysate. **B)** IFNα treatment induces proteasome-dependent degradation of NEK1^t in HEK293 cells. MG132: proteasome inhibitor, n=3. **C)** *PML* silencing impedes IFNα-induced NEK1^t degradation. Quantifications (right), n=3. **D)** Western blot of NEK1^t protein from the spinal cord of

age-matched *Nek1*$^{t/t}$ or *Nek1*$^{t/t}$ *Pml*$^{-/-}$ mice following IFNα or poly(I:C) therapy, (*) non-specific band. **E)** IFNα or poly(I:C) therapy eliminates NEK1^{t} aggregates in αMNs of *Nek1*$^{t/t}$ mice. Quantifications: ≥30 αMNs from ≥3 mice **F)** IFNα or poly(I:C) therapies selectively extend lifespan in *Pml*-proficient *Nek1*$^{t/t}$ mice. Arrowhead: therapy initiation, continued until death. **G)** IFNα or poly(I:C) therapies improve muscle strength and neuromuscular function selectively in *Pml*-proficient *Nek1*$^{t/t}$ ALS mice. Trendlines in Supplementary Fig.S2E.

Figure 1

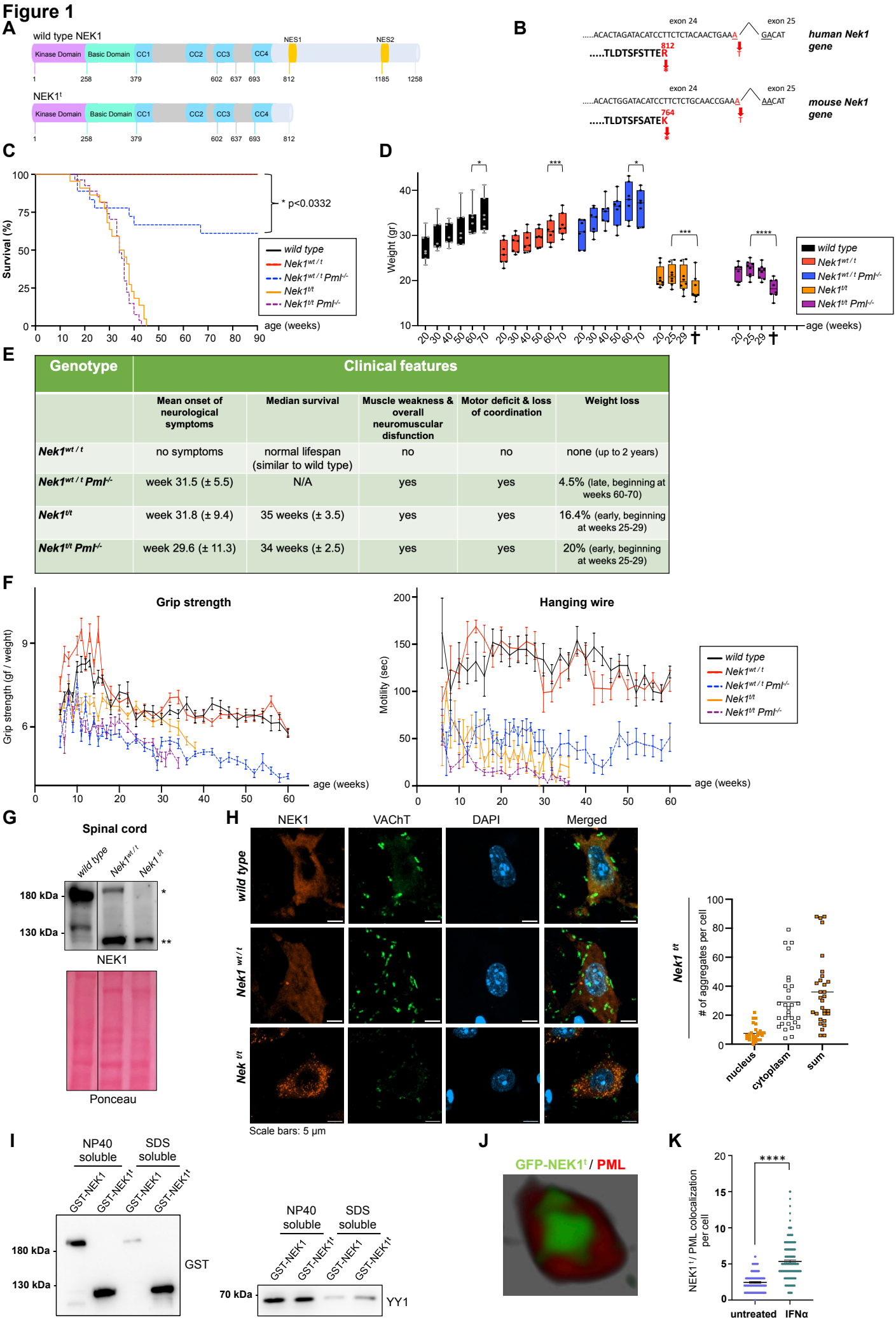
A
wild type NEK1
Kinase Domain
Basic Domain
CC1
CC2
CC3
CC4
NES1
NES2
1
258
379
602
637
693
812
1185
1258
NEK1t
B
exon 24
exon 25
.....ACACTAGATACATCCTTCTCTACAACTGAAA
GACAT
human Nek1 gene
.....TLDTSFSTTER
812
.....ACACTGGATACATCCTTCTCTGCAACCGAAA
AACAT
mouse Nek1 gene
.....TLDTSFSATEK
764
C
Survival (%)
* p<0.0332
wild type
Nek1wt/t
Nek1wt/t Pml-/-
Nek1t/t
Nek1t/t Pml-/-
age (weeks)
D
Weight (gr)
age (weeks)
E
Genotype
Clinical features
Mean onset of neurological symptoms
Median survival
Muscle weakness & overall neuromuscular disfunction
Motor deficit & loss of coordination
Weight loss
Nek1wt/t
no symptoms
normal lifespan (similar to wild type)
no
no
none (up to 2 years)
Nek1wt/t Pml-/-
week 31.5 (± 5.5)
N/A
yes
yes
4.5% (late, beginning at weeks 60-70)
Nek1t/t
week 31.8 (± 9.4)
35 weeks (± 3.5)
yes
yes
16.4% (early, beginning at weeks 25-29)
Nek1t/t Pml-/-
week 29.6 (± 11.3)
34 weeks (± 2.5)
yes
yes
20% (early, beginning at weeks 25-29)
F
Grip strength
Grip strength (gf / weight)
age (weeks)
Hanging wire
Motility (sec)
age (weeks)
G
Spinal cord
wild type
Nek1wt/t
Nek1t/t
180 kDa
130 kDa
NEK1
Ponceau
H
NEK1
VAChT
DAPI
Merged
wild type
Nek1wt/t
Nek t/t
Scale bars: 5 µm
Nek1t/t
# of aggregates per cell
nucleus
cytoplasm
sum
I
NP40 soluble
SDS soluble
GST-NEK1
GST-NEK1t
180 kDa
130 kDa
GST
70 kDa
YY1
J
GFP-NEK1t / PML
K
NEK1t / PML colocalization per cell
untreated
IFNα

Figure 2

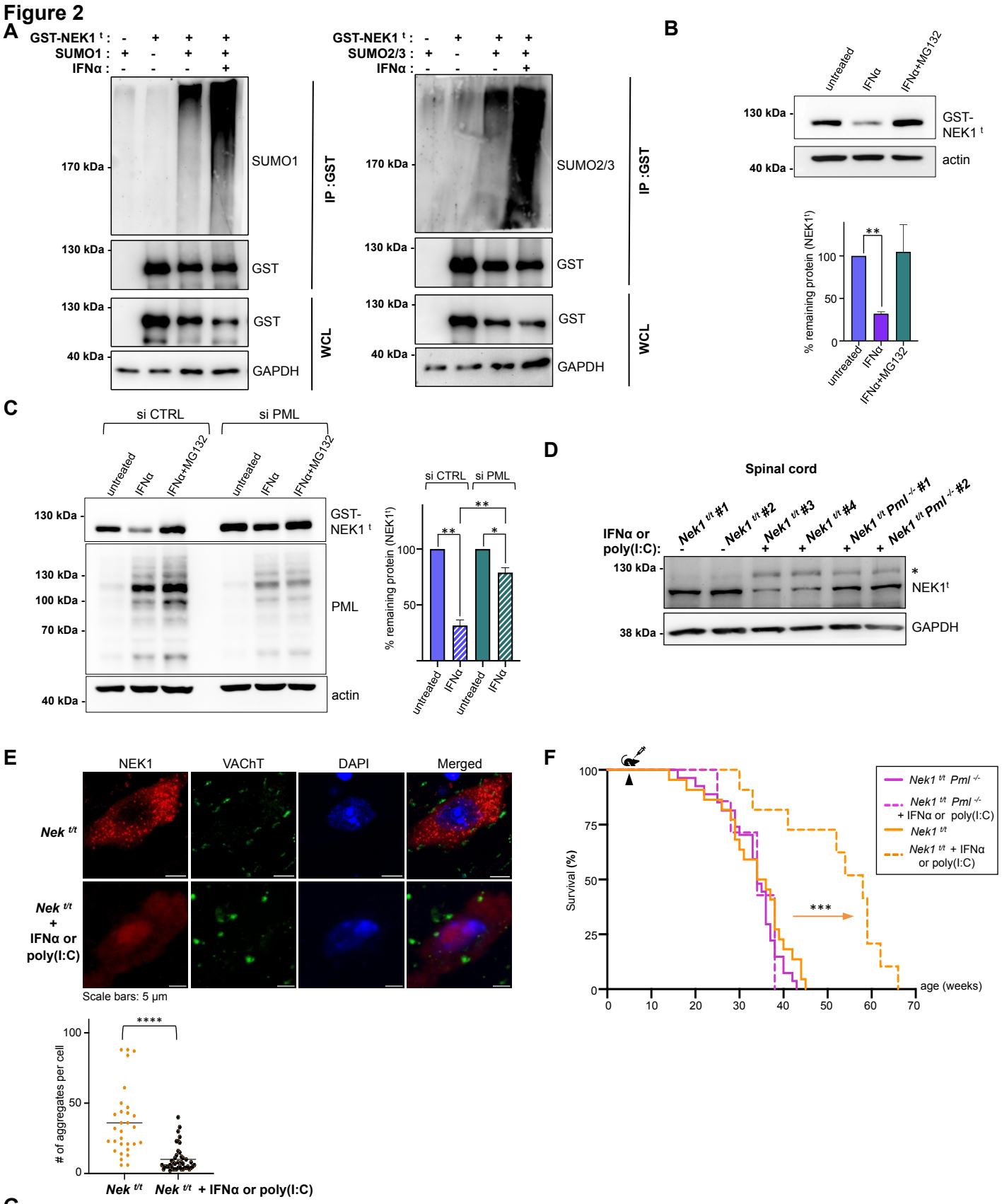
A
GST-NEK1 t :
SUMO1 :
IFNα :
170 kDa
130 kDa
40 kDa
SUMO1
GST
GAPDH
IP :GST
WCL
SUMO2/3
B
untreated
IFNα
IFNα+MG132
GST-NEK1 t
actin
% remaining protein (NEK1t)
C
si CTRL
si PML
100 kDa
70 kDa
PML
D
Spinal cord
IFNα or poly(I:C):
Nek1 t/t #1
Nek1 t/t #2
Nek1 t/t #3
Nek1 t/t #4
Nek1 t/t Pml -/- #1
Nek1 t/t Pml -/- #2
NEK1t
E
NEK1
VAChT
DAPI
Merged
Nek t/t
Nek t/t + IFNα or poly(I:C)
Scale bars: 5 µm
# of aggregates per cell
Nek t/t + IFNα or poly(I:C)
F
Survival (%)
age (weeks)
Nek1 t/t Pml -/-
Nek1 t/t Pml -/- + IFNα or poly(I:C)
Nek1 t/t
Nek1 t/t + IFNα or poly(I:C)
G
Grip strength
Nek1 t/t
Grip strength (gf / weight)
Nek1 t/t Pml-/-